



Monolithic ultra-high-Q lithium niobate microring resonator

MIAN ZHANG,^{1,†} CHENG WANG,^{1,†} REBECCA CHENG,^{1,2} AMIRHASSAN SHAMS-ANSARI,^{1,3} AND MARKO LONČAR^{1,*}

¹John A. Paulson School of Engineering and Applied Sciences, Harvard University, Cambridge, Massachusetts 02138, USA

²Department of Physics, Brown University, Providence, Rhode Island 02912, USA

³Department of Electrical Engineering and Computer Science, Howard University, Washington, DC 20059, USA

*Corresponding author: loncar@seas.harvard.edu

Received 9 November 2017; revised 26 November 2017; accepted 27 November 2017 (Doc. ID 313057); published 18 December 2017

We demonstrate an ultralow loss monolithic integrated lithium niobate photonic platform consisting of dry-etched subwavelength waveguides with extracted propagation losses as low as 2.7 dB/m and microring resonators with quality factors up to 10^7 . © 2017 Optical Society of America under the terms of the [OSA Open Access Publishing Agreement](#)

OCIS codes: (130.3730) Lithium niobate; (230.5750) Resonators; (130.3990) Micro-optical devices.

<https://doi.org/10.1364/OPTICA.4.001536>

Lithium niobate (LN) is a material with a wide range of applications in optical and microwave technologies, owing to unique properties that include large second-order nonlinear susceptibility ($\chi^{(2)} = 30 \text{ pm/V}$), large piezoelectric response ($C_{33} \sim 250 \text{ C/m}^2$), a wide optical transparency window (350 nm to 5 μm), and a high refractive index (~ 2.2) [1]. Conventional LN devices, including fiber-optic modulators and periodically poled frequency converters, have been the workhorse of the optoelectronics industry. Optical waveguides in these components are defined by ion diffusion or proton exchange methods, which result in low index contrast and weak optical confinement. An integrated LN platform, featuring sub-wavelength scale light confinement and dense integration of optical and electrical components, has the potential to revolutionize optical communication and microwave photonics [1–7].

The major roadblock for the practical application of integrated LN photonics is the difficulty of fabricating devices that simultaneously achieve low optical propagation loss and high confinement. Recently developed thin-film LN-on-insulator technology makes this possible, and has resulted in the development of two complementary approaches to define nanoscale optical waveguides: hybrid and monolithic. The hybrid approach integrates an easy-to-etch material (e.g., silicon or silicon nitride) with LN thin films to guide light [2–4] with a relatively low propagation loss (0.3 dB/cm) [4]. However, the resulting optical modes only partially reside in the active material region (i.e., LN), reducing the nonlinear interaction efficiency. The monolithic approach relies on direct etching of LN to achieve high optical confinement

in the active region, but has suffered from a relatively high propagation loss. While freestanding LN microdisk resonators have achieved optical quality factors (Q) of $\sim 10^6$ [5,6], integrated microring resonators typically feature $Q \sim 10^5$ with waveguide propagation loss on the order of 3 dB/cm [7]. Since LN is perceived as a difficult-to-etch material, it is commonly accepted that low-loss propagation in a monolithic waveguide is not possible, and therefore is not the most promising path forward.

Here we challenge the *status quo* and show that sub-wavelength scale lithium niobate waveguides can be fabricated with a propagation loss as low as $2.7 \pm 0.3 \text{ dB/m}$ through an optimized standard etching process. We demonstrate nearly critically coupled ultra-high Q -factor optical cavities with measured $Q_L = 5 \times 10^6$ corresponding to intrinsic $Q_I \sim 10^7$.

We fabricate an integrated waveguide-coupled microring and racetrack resonators with a bending radius $r = 80 \mu\text{m}$, and various straight arm lengths l and waveguide widths w [Fig. 1(a)]. The optical modes in these resonators have different interaction strength with the etched sidewalls, which allows us to identify the source of the optical losses [Fig. 1(b)]. We fabricate the devices using 600 nm thick X-cut LN thin films on 2 μm of silicon dioxide (SiO_2) on silicon substrates (NanoLN). We use standard electron beam lithography to define patterns in hydrogen silsesquioxane (HSQ) resist with multipass exposure. The patterns are subsequently transferred into the LN thin film using a commercial inductively coupled plasma reactive ion etching (ICP RIE) tool. We use Ar^+ plasma to physically etch LN where the plasma power and chamber condition are tuned to minimize surface re-deposition of removed LN and other contaminations present in the chamber. We etch a total of $h_{\text{rib}} = 350 \text{ nm}$ of LN with a bias power of 112 W, leaving a $h_{\text{slab}} = 250 \text{ nm}$ thin LN slab. After cleaning and removal of the resist, the devices are cladded by depositing 1.5 μm of SiO_2 using plasma-enhanced chemical vapor deposition (PECVD).

The optical Q -factors of these resonators are measured using a tunable telecom external cavity diode laser (Santec TSL-510, Komaki, Japan). To calibrate the Q measurement, we modulate (500 MHz) the laser output using an external electro-optic modulator. Figure 2(a) shows a close to critically coupled micro-racetrack resonator with a loaded (intrinsic) Q -factor of 5.0 (10.0 ± 0.7) million at an optical excitation wavelength of 1590 nm.

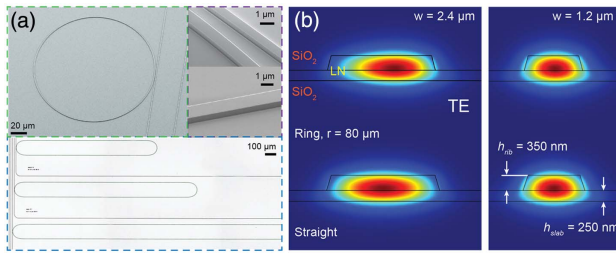


Fig. 1. (a) Scanning electron microscope (top) and optical microscope (bottom) images of a microring and micro-racetrack resonators of various lengths. Inset: Close-up of the etched waveguides. (b) Simulated optical modes in straight and bent waveguides.

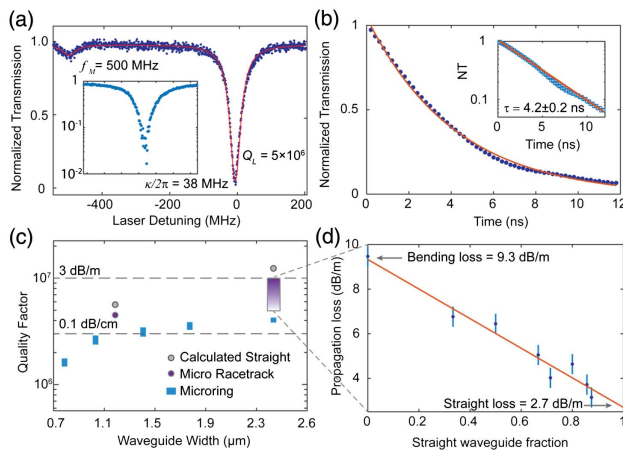


Fig. 2. (a) Resonance linewidth in the best devices is as narrow as 38 MHz, corresponding to loaded $Q_L = 5 \times 10^6$. The laser is modulated by a precise frequency source at 500 MHz for calibration. Inset: Transmission spectrum in logarithmic scale indicating that the resonator is nearly critically coupled. (b) Ring-down measurement of the same device. (c) Measured quality factors for different resonators on several chips. (d) Extracted propagation loss for racetrack resonators. All the measurements are conducted around 1590 nm.

To confirm the Q -factor, we directly ascertain the photon lifetime of the resonator using ring-down measurements [Fig. 2(b)]. The fitted data show a lifetime of 4.2 ± 0.2 ns in good agreement with the spectral measurements.

We show that sidewall scattering is still a significant loss channel in our devices by investigating structures with different waveguide widths. Figure 2(c) shows the intrinsic Q measured for fabricated ring and racetrack resonators. Increasing the waveguide width from 800 nm to $2.4 \mu\text{m}$ leads to a Q improvement from ~ 1.5 to ~ 4 million. This improvement is expected from the reduced interaction of the light and the etched sidewalls [Fig. 1(b)].

We extract the straight optical waveguide propagation loss by comparing the optical Q -factors of micro-racetrack resonators with different straight section lengths from 0 to 14 mm, with the same waveguide width of $2.4 \mu\text{m}$ and a bending radius of $80 \mu\text{m}$. Indeed, racetrack resonators with longer straight sections exhibit higher optical Q -factors, because light in the straight section interacts less with the sidewall scattering centers than in the bending region [Fig. 1(b)]. The results are shown in Fig. 2(d), where we extract a straight waveguide loss of 2.7 ± 0.3 dB/m

from the intersection of the fitted line. The extracted bending loss of 9.3 ± 0.9 dB/m agrees well with the measurements in ring resonators. By comparing the straight section loss of two racetrack resonators with different widths (1.2 and $2.4 \mu\text{m}$) and using numerical modeling, we estimate an upper bound of 1.5 dB/m for the intrinsic loss of our platform. The possible contributing factors are ion-implantation damage introduced during the LN thin-film production process, top-surface roughness due to LN polishing, and finite PECVD SiO_2 cladding absorption. Importantly, these loss mechanisms could be mitigated by a combination of defects annealing and finer top-surface polishing [8]. We expected the loss contributions of the monolithic LN platform could be further reduced toward its material intrinsic loss limit of <0.1 dB/m [1].

In conclusion, we show that the monolithic LN nanophotonic platform is a viable path forward. The ultralow loss, high optical confinement and tight bending radius combined with the ability to integrate microwave electrodes [7] will bring electro-optic [2,7] and nonlinear optical [4] systems into a new design parameter space that has been inaccessible until now. This could enable a wide range of applications, including those in ultralow-loss quantum photonics [9], coherent microwave-to-optical conversion [10,11], and active topological photonics [12]. We emphasize that the LN device layer sits atop a standard silicon handle wafer and our platform therefore can also be integrated with many existing photonic technologies. Finally, we hope that our work will stimulate further activities and a renewed interest in monolithic LN nanophotonics, which could ultimately lead to the development of dedicated LN nanofabrication foundries and/or the introduction of etched LN into existing silicon photonics processes.

Funding. National Science Foundation (NSF) (ECCS-1609549, DMR-1231319); Office of Naval Research (ONR) MURI (N00014-15-1-2761); REU Program; Harvard University Office of Technology Development Physical Sciences and Engineering Accelerator; Army Research Laboratory (ARL) (W911NF1520067).

[†]These authors contributed equally to this work.

REFERENCES

1. L. Maleki and A. Matsko, *Ferroelectric Crystals for Photonic Applications* (Springer, 2009).
2. L. Chen, Q. Xu, M. G. Wood, and R. M. Reano, *Optica* **1**, 112 (2014).
3. A. Rao, A. Patil, J. Chiles, M. Malinowski, S. Novak, K. Richardson, P. Rabiei, and S. Fathpour, *Opt. Express* **23**, 22746 (2015).
4. L. Chang, Y. Li, N. Volet, L. Wang, J. Peters, and J. E. Bowers, *Optica* **3**, 531 (2016).
5. R. Luo, H. Jiang, S. Rogers, H. Liang, Y. He, and Q. Lin, *Opt. Express* **25**, 24531 (2017).
6. J. Wang, F. Bo, S. Wan, W. Li, F. Gao, J. Li, G. Zhang, and J. Xu, *Opt. Express* **23**, 23072 (2015).
7. C. Wang, M. Zhang, B. Stern, M. Lipson, and M. Loncar, "Nanophotonic lithium niobate electro-optic modulators," arXiv: 1701.06470 (2017).
8. X. Ji, F. Barbosa, S. Roberts, A. Dutt, J. Cardenas, Y. Okawachi, A. Bryant, A. Gaeta, and M. Lipson, *Optica* **4**, 619 (2017).
9. J. O'Brien, *Science* **318**, 1567 (2007).
10. C. Javerzac-Galy, K. Plekhanov, N. R. Bernier, L. D. Toth, A. K. Feofanov, and T. J. Kippenberg, *Phys. Rev. A* **94**, 053815 (2016).
11. M. Soltani, M. Zhang, C. Ryan, G. J. Ribeill, C. Wang, and M. Loncar, *Phys. Rev. A* **96**, 043808 (2017).
12. Q. Lin, M. Xiao, L. Yuan, and S. Fan, *Nat. Commun.* **7**, 13731 (2016).